Evaluation of Active Control Concepts for a Self-adjusting Membrane-type Acoustic Metamaterial

Felix Langfeldt*, Jordan Cheer

Institute of Sound and Vibration Research, University of Southampton, Southampton, SO17 1BJ, United Kingdom

* *E-mail: F.Langfeldt@soton.ac.uk*

Introduction

Membrane-type acoustic metamaterials (MAM), as first proposed by Yang et al. [1], consist of a thin pre-stressed membrane with periodically attached masses. By carefully tuning the material and geometrical properties of the membrane and the added masses, the low-frequency sound transmission loss (TL) of MAM can exhibit so-called anti-resonances with TL values that are much larger than the corresponding mass-law values. This makes MAM a very promising solution for tackling low-frequency tonal noise using lightweight materials. A big drawback of MAM is that the anti-resonance frequencies cannot be changed, once the MAM has been manufactured. The bandwidth of MAM is typically very small, which makes it difficult to apply MAM to problems where either the tonal frequencies of the noise sources change, or where the properties of the membrane change, e.g. due to thermal expansion.

Motivated by this shortcoming, many different techniques for changing the MAM anti-resonance frequencies after manufacturing have been proposed in the literature, for example using electric fields [2] or pressurization leading to non-linear deformation [3]. While these investigations could clearly demonstrate that it is possible to substantially change the anti-resonance frequencies of MAM using these techniques, it has not been shown whether these approaches are able to adapt the tuning frequency to a noise source with changing tonal frequencies.

This paper presents a preliminary numerical investigation of a new kind of adjustable MAM, which uses different active control algorithms to control a noise source with tonal frequencies that change over time. First, the general set-up of the adjustable MAM is described briefly. Then, the numerical model used to evaluate the sound transmission loss of the MAM is presented. The active control algorithms investigated here are discussed afterwards. In the subsequent section, the simulation results are presented. Finally, it is discussed using additional simulation results how the performance of the adjustable MAM changes in a multi-celled array when not all unit cells are actively controllable in order to reduce the required number of actuators.

Set-up of the self-adjusting MAM

Fig. 1 shows a 3D view of the membrane-type acoustic metamaterial with added masses arranged in a square periodic lattice. Note that the unit cells (one unit cell being highlighted in Fig. 1) are not bounded by a grid

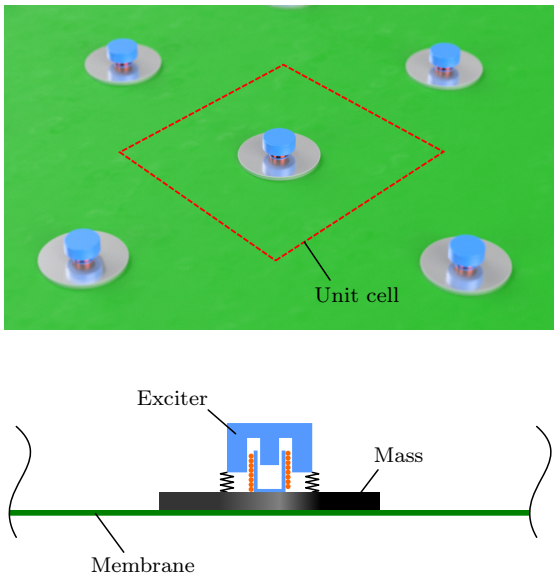

Figure 1: Illustration of the self-adjusting membrane-type acoustic metamaterial. Top: 3D view with emphasis of a single unit cell; Bottom: Cross-section of the unit cell with the different components.

structure and the metamaterial is assumed to extend infinitely within its plane. The MAM consists of a 100 µm thick polyester (PET) film with a circular mass attached to the center of each unit cell. The membrane is pretensioned by an isotropic in-plane stress resultant of 200 N/m. The unit cell size of the MAM considered here is 30 mm × 30 mm. The diameter of the added mass made of aluminium is 10 mm and its thickness is 0.5 mm.

To actuate the MAM and make the self-adjustment possible, an electrodynamic exciter is attached to each mass. The exciter consists of a base, which is fixed to the mass, a moving mass, a suspension, and a voice coil which can be driven by an electric signal to exert a force on the moving mass and base of the exciter.

Numerical model

A single unit cell of the MAM is modelled using finite elements. The membrane is represented by 2D shell elements and the added mass is modelled using 3D solid elements. On both sides of the MAM, 3D acoustic elements are used to model the fluid (air) and full vibro-acoustic coupling is enforced in the simulations. The fluid domains are truncated using perfectly matched layers to minimize reflections at the terminations. The lateral boundaries of the membrane and the fluid are spec-

ified as periodic boundaries to make the unit cell part of an infinite planar array of MAM unit cells. The acoustic excitation is prescribed as a normally incident plane acoustic wave with amplitude p_i and the sound pressures and sound powers on each side of the MAM are evaluated to quantify the sound transmission behavior of the MAM. Table 1 provides an overview of the material parameters used in the simulations. The speed of sound and density of the air were set to 340 m/s and 1.2 kg/m^3, respectively.

The exciter is represented by a coupled lumped mechanical and electrical system [4]. In the time-domain, the governing equations are as follows:

$$M_\mathrm{ms}\ddot{w}_\mathrm{ms} + D_\mathrm{ms}\dot{w}_\mathrm{ms} + \frac{1}{C_\mathrm{ms}} w_\mathrm{ms} = D_\mathrm{ms}\dot{w}_\mathrm{b} + \frac{1}{C_\mathrm{ms}} w_\mathrm{b} + B\ell I, \quad (1)$$

where w_ms is the displacement of the moving mass M_ms, D_ms and C_ms are the mechanical damping and compliance of the suspension, w_b is the displacement of the exciter base, and $B\ell$ is the force factor. The current I acting across the voice coil of the exciter is governed by

$$L_\mathrm{e}\dot{I} + R_\mathrm{e} I = U - B\ell\left(\dot{w}_\mathrm{ms} - \dot{w}_\mathrm{b}\right), \quad (2)$$

where L_e and R_e are the inductance and resistance of the exciter and U is the excitation voltage. Finally, the base force F_b exerted by the exciter onto the host structure is given by

$$F_\mathrm{b} = -M_\mathrm{b}\ddot{w}_\mathrm{b} - M_\mathrm{ms}\ddot{w}_\mathrm{ms}, \quad (3)$$

where M_b is the mass of the exciter base structure. The lumped parameters of the exciter used in the simulations are given in Table 2.

The finite element model of the MAM is coupled with the lumped model of the exciter by applying the base force F_b to the center of the added mass and enforcing the base displacement w_b to be equal to the transversal displacement of the center of the added mass.

Table 1: Material parameters used in the simulations.

	Membrane	Mass	
Material	PET	Aluminium	
Density	1310	2700	$\frac{\mathrm{kg}}{\mathrm{m}^3}$
Young's modulus	2.3	70	GPa
Poisson's ratio	0.4	0.33	—
Loss factor	1	0	%

Table 2: Mechanical and electrical parameters for the exciter.

M_b	M_ms	D_ms	C_ms	L_e	R_e	$B\ell$
1 g	2 g	50 $\frac{\mathrm{mN\,s}}{\mathrm{m}}$	5 $\frac{\mathrm{mm}}{\mathrm{N}}$	0.1 mH	8 Ω	1 T m

Control algorithms

In this section two control algorithms for adjusting the active MAM to a tonal frequency in the incident noise spectrum are presented.

Feed forward incident pressure control

The first approach to controlling the anti-resonance frequency of the MAM considered here is to feed the sound pressure measured on the incident side of the MAM p_1 through an adjustable gain K back into the exciter (as shown in Fig. 2). This is shown exemplarily in Fig. 3 using simulations with different values of the gain K.

A simple way to exploit this and achieve a self-adjusting MAM is to add a peak detection algorithm (e.g. using a Fast Fourier Transform) and identify the tonal frequency dominating the incident noise field p_1. This tonal frequency corresponds to the target anti-resonance frequency f_P that the MAM needs to be tuned to. The gain K can be adjusted based on a look-up table which provides a relationship of $K(f_\mathrm{P})$ for the given MAM and exciter combination. This relationship depends on the properties of both the MAM and the exciter and has been pre-computed using simulations in the considered case. The result is shown in Fig. 4.

Filtered-X LMS algorithm (FxLMS)

FxLMS is an adaptive filter algorithm that is widely employed in active noise control [5]. The FxLMS algorithm is applied to the adjustable MAM as shown in Fig. 5. The measured reference pressure signal p_1 is passed through a digital finite impulse response (FIR) filter F to generate

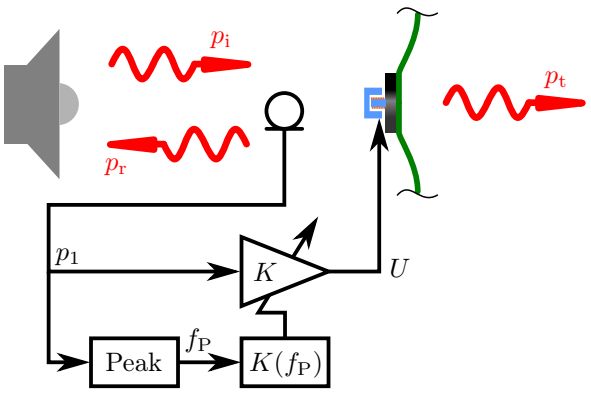

Figure 2: Control set-up using an adjustable feed forward gain K and peak frequency identification.

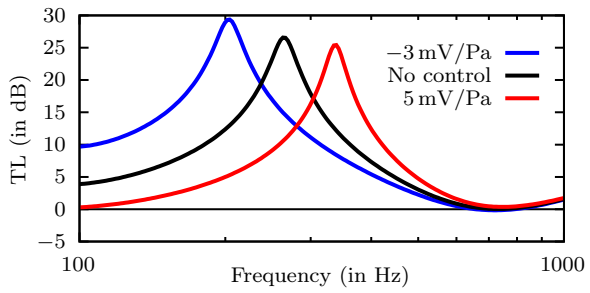

Figure 3: Sound transmission loss of the active MAM shown in Fig. 2 for different values of the feed forward gain K.

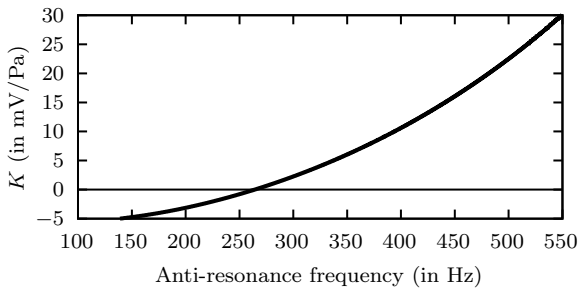

Figure 4: Simulated relationship between the desired anti-resonance frequency f_P of the MAM and the required feed forward gain K.

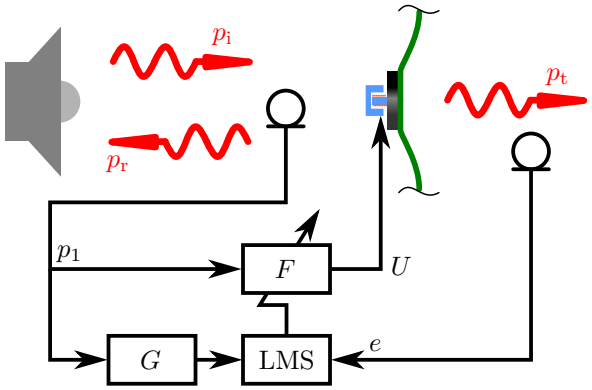

Figure 5: Control set-up using an adaptive filter F and the FxLMS algorithm.

the voltage signal U to drive the exciter. The coefficients of the filter F are adapted using the LMS algorithm in order to minimize the error signal e at the error microphone on the transmission side in a least-mean-squares sense. Since the secondary path from the exciter voltage U to the transmitted sound pressure p_t is affected by the dynamics of the adjustable MAM, these secondary path dynamics need to be taken into account when feeding the reference signal p_1 into the LMS algorithm by filtering p_1 with a plant model G. For the investigations in this paper, the plant model G has been represented by a finite impulse response filter with an order of $N = 50$. The filter coefficients have been estimated using the simulation model, so it is a perfect estimate of the physical response.

Results

The aforementioned control algorithms have been implemented in a SIMULINK model where the response of the MAM (i.e. the radiated sound pressure p_t) to the acoustical and electrical excitation has been modelled based on the FEM model. In these simulations, the amplitude of the incident sound field p_i is time-dependent: It consists of a tone with frequency f_T superimposed with white noise and a tone-to-noise-ratio of 20 dB. The tonal frequency f_T varies over time as follows: Initially, $f_\mathrm{T} = 265\,\mathrm{Hz}$ (corresponding to the anti-resonance frequency of the passive MAM). After 4 s, f_T decreases linearly to 150 Hz at 10 s. The tonal frequency stays at this value for 5 s and then increases linearly to 450 Hz at 25 s, after which f_T remains constant at this frequency.

Fig. 6(a) shows the spectrogram of the sound level of the transmitted sound wave in the case of the passive MAM without self-adjustment. Since the anti-resonance of the MAM does not change over time (visible as the dark area in the spectrogram), the tone clearly dominates the spectrum as soon as f_T is lower or higher than 265 Hz. The results for the self-adjusting MAM with feed forward incident pressure control are shown in Fig. 6(b). In this set-up, the MAM is capable of tracking the tonal frequency and updating the gain K such that $f_\mathrm{P} \approx f_\mathrm{T}$. The sound level of the tone is clearly attenuated over the whole time span. Finally, Fig. 6(c) shows the spectrogram for the MAM controlled using the FxLMS adaptive filter. Generally, the tonal frequency is effectively eliminated using this approach and—since the adaptive filter uses 20 coefficients—the background noise is also reduced compared to the other two cases. On the other hand, the FxLMS algorithm is more computationally demanding and requires an error microphone on the transmission side of the MAM.

Multi-celled MAM array

The results presented in the previous section demonstrate the capability of the MAM to adjust itself to a changing noise field, either by using an adaptive feed forward gain or using an adaptive filter with FxLMS. In practice it will be infeasible to actuate an exciter in every single unit cell of the MAM. For the given MAM unit cell, this would mean attaching, wiring, and controlling over 1000 actuators per m^2.

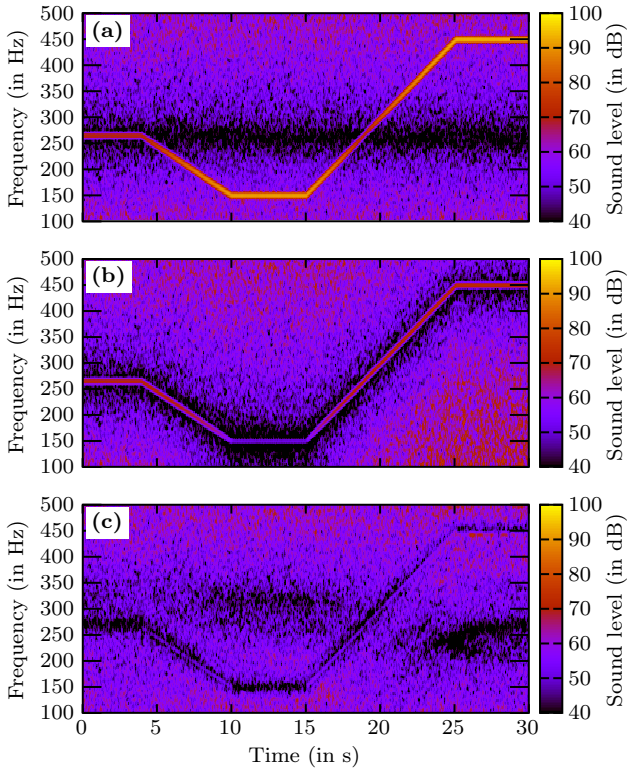

Figure 6: Simulated spectrograms of different MAM configurations under time-varying tonal excitation with background noise. (a) Passive MAM; (b) Feed forward incident pressure control; (c) FxLMS adaptive filter.

Using the simulation model it is investigated how the performance of the self-adjusting MAM is changed when only a fraction of the MAM unit cells are controllable. The simulation model has been modified to comprise of an array of $N \times M$ unit cells. Within this super-cell only one unit cell contains an active exciter. In all other unit cells the electrical terminals of the exciter are open (i.e. current $I = 0$). Thus, the active unit cell fraction is given by $\phi = 1/(NM)$. Fig. 7(a) shows simulation results for feed forward pressure control with a fixed gain of $K = 10\,\mathrm{mV/Pa}$ and different values of ϕ. As the active unit cell fraction decreases, the anti-resonance frequency shifting due to the feed forward pressure control decreases as well. This can be explained by a single active unit cell being essentially in parallel to $NM - 1$ passive unit cells with unchanged anti-resonance frequencies. Therefore, the frequency shifting effect diminishes when more and more passive unit cells are surrounding the active unit cell.

One way to mitigate this in an approximate manner is to scale the gain K by the total number of unit cells in one super-cell. Fig. 7(b) shows the simulated transmission loss with a compensated gain of $K = NM \cdot 10\,\mathrm{mV/Pa}$. It can be seen that using this compensation the anti-resonance frequency is almost the same in all four cases. Therefore, it is possible to use a small active unit cell fraction in order to reduce manufacturing effort and cost. However, it should be noted that there are likely to be limitations to this approach, for example, very high gains can lead to non-linearities in the exciter and a reduction in performance. Also, the super-cell should be smaller than the acoustic wavelength for the parallel connection analogy to be valid.

Conclusions

Numerical studies of a self-adjusting membrane-type acoustic metamaterial have been presented in this paper.

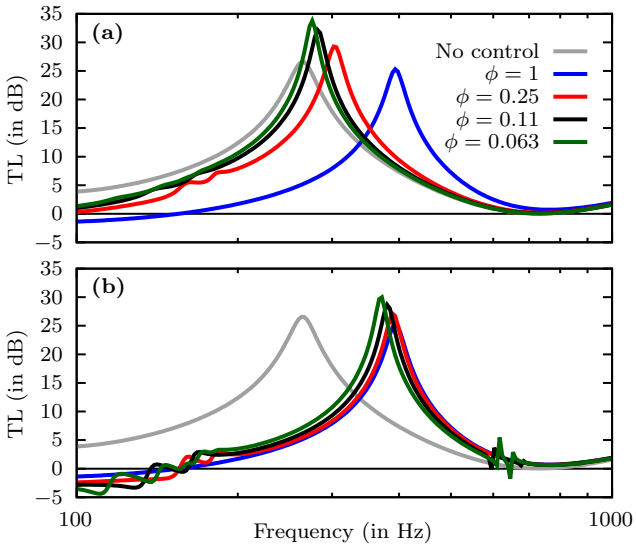

Figure 7: Simulated sound transmission loss of a multi-celled ($N \times M$) MAM with different active unit cell fractions ϕ and feed forward incident pressure control. (a) Constant gain $K = 10\,\mathrm{mV/Pa}$; (b) Compensated gain $K = NM \cdot 10\,\mathrm{mV/Pa}$.

The MAM is actuated using an electrodynamic exciter attached to the added mass and two active control algorithms have been investigated: Feed forward control using the incident sound pressure and an adjustable gain as well as an adaptive filter based on the FxLMS algorithm. It could be demonstrated that by adjusting the gain, the anti-resonance frequency of the MAM can be actively controlled to track a changing tonal frequency in the incident noise spectrum. The FxLMS algorithm offers an even more efficient attenuation of a time-varying tone as well as some additional broadband attenuation, at the cost of an additional error microphone and slightly higher complexity. Additional simulations of multi-celled MAM with only a fraction of the unit cells being controllable indicated that the proposed concept still works when compensating for the reduced actuator density. This can be useful for minimizing the number of required actuators and reducing the complexity of adjustable MAM designs.

The presented results constitute first preliminary steps and further properties of the adjustable MAM concepts, such as robustness, non-linearities of the actuation, power consumption, or optimization potentials will be explored in ongoing research.

Acknowledgements

F. Langfeldt's research was funded by the Deutsche Forschungsgemeinschaft (DFG, German Research Foundation) in the framework of the Walter Benjamin Programme (grant no. 455631459).

The authors acknowledge the use of the IRIDIS High Performance Computing Facility, and associated support services at the University of Southampton, in the completion of this work.

References

[1] Yang, Z., Mei, J., Yang, M., Chan, N. H., and Sheng, P.: Membrane-Type Acoustic Metamaterial with Negative Dynamic Mass. Physical Review Letters 101(20) (2008), p. 204301.

[2] Xiao, S., Ma, G., Li, Y., Yang, Z., and Sheng, P.: Active Control of Membrane-Type Acoustic Metamaterial by Electric Field. Applied Physics Letters 106 (2015), p. 091904.

[3] Langfeldt, F., Riecken, J., Gleine, W., and von Estorff, O.: A Membrane-Type Acoustic Metamaterial with Adjustable Acoustic Properties. Journal of Sound and Vibration 373 (2016), pp. 1–18.

[4] Fahy, F. and Gardonio, P.: Sound and Structural Vibration. 2nd ed. Academic Press, Oxford, 2007.

[5] Elliott, S. J.: Signal Processing for Active Control. Academic Press, London, 2001.